Published in final edited form as:
Cardiovasc Res. 2012 July 1; 95(1): 69–76. doi:10.1093/cvr/cvs164.

In Vivo Alterations in Cardiac Metabolism and Function in the Spontaneously Hypertensive Rat Heart

Michael S. Dodd, MBiochem, **Daniel R. Ball, MChem**, **Marie A. Schroeder, DPhil**, **Lydia M. Le Page, MChem**, **Helen J. Atherton, PhD**, **Lisa C. Heather, DPhil**, **Anne-Marie Seymour, PhD**, **Houman Ashrafian, MD, DPhil**, **Hugh Watkins, MD, PhD, FRCP, FMed Sci**, **Kieran Clarke, PhD**, and **Damian J. Tyler, PhD**
Department of Physiology, Anatomy and Genetics, University of Oxford, Oxford, UK (M.S.D., D.R.B., M.A.S., L.M.L.P., H.J.A., L.C.H., K.C., D.J.T.), the Department of Cardiovascular Medicine, University of Oxford, Oxford, UK (M.S.D., H.A., H.W.), and the Department of Biological Sciences, University of Hull, Hull, UK (A-M.S)

Introduction

The World Health Organisation estimates that in 2004, 7.2 million people died worldwide from coronary heart disease[1]. A major risk factor for coronary heart disease is hypertension. This is characterized by an increase in arterial blood pressure and a subsequent increase in left ventricular (LV) wall stress. To protect the hypertensive heart, pro-hypertrophic factors increase LV wall thickness and equalize wall stress via the LaPlace law[2]. However, if left untreated the heart will ultimately fail due to an inability to maintain normal cardiac output[2].

In the healthy heart, β-oxidation contributes 60-80% of ATP[3,4]. The remaining 20-40% is derived from carbohydrate metabolism, principally the metabolism of glucose and lactate. However β-oxidation and glucose oxidation are dynamically regulated to provide the most efficient energy production with the most abundant fuel[5]. This ensures the heart can continue to function under changing metabolic environments. Recent evidence suggests that many forms of heart disease are linked to alterations in cardiac metabolism[6]. For example, it has been suggested that in the hypertrophied heart there are changes in the profile of substrate utilization, limiting energy provision and eventually leading to a deterioration in heart function[6,7].

Spontaneously hypertensive rats (SHRs) are used as a model of hypertension and hypertrophy[8,9]. The combination of hypertension and hypertrophy result in continuing adaptation of cardiac metabolism[8,9]. During early development of hypertension (5-10 weeks), the SHR heart displays compensated alterations in glycolytic intermediates and high energy phosphates, which lead to a normalized myocardial energy state[9]. At 15 weeks of age

Address for correspondence: Dr Damian Tyler PhD, Department of Physiology, Anatomy & Genetics, Sherrington Building, University of Oxford, Parks Road, Oxford, UK, OX1 3PT, Fax: +44 (0)1865 282272, Tel: +44 (0)1865 282252, damian.tyler@dpag.ox.ac.uk.

Disclosers
Equipment support was provided by General Electric Healthcare (Amersham, UK).

Europe PMC Funders Author Manuscripts

SHRs represent an early compensatory disease model of hypertrophy with elevated blood pressure and concentric hypertrophy[10].

The SHR has a number of genetic mutations which contribute to the hypertensive phenotype. A major mutation is a loss of function of fatty acid translocase (FAT/CD36), a sarcolemmal fatty acid transporter[11]. FAT/CD36 is crucial for the transport of long chain fatty acids (LCFA) across the plasma membrane. Studies in the CD36-deficient mouse have revealed a significant increase in basal glycolysis and glucose uptake in the heart[12]. Fatty acid uptake and oxidation are also severely impaired in these mice, resulting in elevated plasma free fatty acids (FFA) and triglycerides[12]. This is mimicked in the SHR rat at 15 weeks where ^{13}C magnetic resonance spectroscopy (MRS) on the perfused *ex vivo* SHR heart has been used to track a reduction in ^{13}C label incorporation into the TCA cycle from fatty acids[13]. Furthermore, using the radioactive fatty acid analogue, BMIPP (^{123}I-β-methylp-iodophenylpentadecanoic acid), a significant reduction in fatty acid uptake and oxidation was observed in the SHR, similar to the $CD36^{-/-}$ mouse[14]. This *in vitro* evidence demonstrates a major shift in cardiac metabolism away from β-oxidation in the 15 week old SHR heart[13,14].

At this age, the SHR also shows a significant 60% reduction in the inducible pyruvate dehydrogenase (PDH) kinase (PDK)4 mRNA expression[15]. PDK4 is one of the key regulatory enzymes of PDH in the heart. In type-1 diabetes and high fat feeding, elevated mRNA and protein expression of PDK4 has been shown to decrease both *in vitro* PDH activity and *in vivo* PDH flux[16-19]. Thus, given the decrease in PDK4 in the SHR heart, we would hypothesise that *in vivo* PDH flux would be increased.

Progression into sustained hypertension and hypertrophy shows that by 25 weeks the SHR heart has a reduced lactate/pyruvate ratio and altered high energy phosphate levels, indicative of perturbed energy homeostasis[9]. As the SHR heart ages to 16-18 months, the animals display severe insulin resistance and increasingly compromised cardiac energetics[20].

The nature of hypertension and hypertrophy mean that there are a multitude of factors affecting disease progression and severity. This is particularly difficult to mimic using *ex vivo* models. Only the *in vivo* setting provides the correct balance of hormonal, functional and regulatory responses to fully characterize the disease. ^{13}C MRS is particularly suited to the study of metabolism in the heart due to the extensive range of metabolites that can be observed[13], but suffers from an inherently low sensitivity which has limited *in vivo* applications. However, this low sensitivity can be overcome using hyperpolarized ^{13}C MRS[21-23]. Hyperpolarization, via dynamic nuclear polarization (DNP) increases the sensitivity of ^{13}C MRS upwards of 10,000-fold over conventional methods[21]. A hyperpolarized compound can be injected *in vivo* and its metabolism visualized in real time[21]. For example, *in vivo* hyperpolarized [1-^{13}C]pyruvate flux through PDH into [^{13}C]bicarbonate and $^{13}CO_2$ has been shown to accurately reflect PDH activity[16]. [1-^{13}C]pyruvate is also processed into [1-^{13}C]lactate and [1-^{13}C]alanine, via lactate dehydrogenase (LDH) and alanine aminotransferase (AAT), respectively. In contrast to [1-^{13}C]pyruvate, [2-^{13}C]pyruvate is able to probe the entry of pyruvate derived acetyl-CoA

into the TCA cycle via visualization of [1-^{13}C]acetylcarnitine, [1-^{13}C]citrate and [5-^{13}C]glutamate[24,25].

In this study our aim was to determine *in vivo* flux through PDH in the SHR heart at a compensated stage of hypertrophy to investigate the balance between anaerobic glycolytic metabolism and glucose oxidation *in vivo.* The findings of this work were supported by *in vivo* cine-MRI measurements of heart function and mass, and *in vitro* biochemical assays of enzyme activity and protein expression.

Methods

[1-^{13}C] and [2-^{13}C]pyruvic acid were obtained from Sigma Aldrich (Sigma-Aldrich Company Ltd. Dorset, UK). Fifteen week old male spontaneously hypertensive rats (SHR) (~300g, n=13) and male Wistar (275-325g, n=11) control rats were obtained from Harlan UK. All animals were housed on a 12:12-hour light–dark cycle and studies were performed between 7a.m.-1p.m., during the early absorptive (fed) state. All investigations conformed to Home Office Guidance on the Operation of the Animals (Scientific Procedures) Act (HMSO) of 1986, to institutional guidelines and the Directive 2010/63/EU of the European Parliament. Experiments were also approved by a local university ethics review board.

Animal handling

Anaesthesia was induced by 2.5-3% isofluorane in oxygen and nitrous oxide (4:1, total of 2l/min). Adequacy of anaesthesia was initially based on loss of pedal response and was then continuously monitored through evaluation of the heart and respiration rate. Anaesthesia was maintained by means of 2% isofluorane delivered during the experiment (O_2:NO_2 4:1, total of 2l/min). When required, a tail vein cannulation for intravenous administration of hyperpolarized solutions was performed before the animals were subsequently placed in a home-built MR animal-handling system[26]. ECG, respiration rate and body temperature were monitored throughout the experiment and air heating was provided to maintain body temperature at 37°C as previously described[17]. Animals fully recovered following anaesthesia for serial MR experiments measurements.

Cine magnetic resonance imaging

Animals were initially imaged to assess left ventricular mass (LVM) and cardiac function. They were positioned in an 11.7T vertical bore MR scanner (Magnex scientific, Oxon UK) interfaced to a Bruker Avance console (Bruker Medical, Ettlingen Germany) and a shielded gradient system (Magnex scientific, UK). A 60mm birdcage transmit/receive RF coil was used to obtain MR images (Rapid biomedical, Rimpar Germany). Experiments were carried out as previously described[27]. Sequences were ECG-triggered and 28–40 frames were collected per cardiac cycle. Left ventricular volumes were derived using the free-hand draw function in ImageJ (NHI, USA). For each heart, LVM, ejection fraction, stroke volume and cardiac output were calculated. Hypertrophy was assessed as an increase in LVM compared to control animals.

A high temporal resolution (HTR) cine-MRI sequence was used to measure diastolic peak ejection and filling rates in SHR and control animals[28]. Briefly, after acquisition of the

conventional cine-MRI sequences, a mid-papillary slice was selected and imaged using HTR cine-MRI over two consecutive cardiac cycles. Chamber volume was measured in every frame after threshold adjustment, using ImageJ. This was then plotted as a function of time and early and late peak filling rates were calculated.

Pyruvate polarization and dissolution

Approximately 40mg of [1-^{13}C]pyruvic acid or [2-^{13}C]pyruvic acid, doped with 15mM trityl radical (OXO63, GE Healthcare) and 3μl Dotarem (1:50 dilution, Guerbet, Birmingham, UK), was hyperpolarized in a polarizer, with 45min of microwave irradiation as previously described[21]. The sample was subsequently dissolved in a pressurized and heated alkaline solution, containing 2.4g/L sodium hydroxide and 100mg/L EDTA dipotassium salt (Sigma-Aldrich), to yield a solution of 80mM hyperpolarized sodium [1-^{13}C]pyruvate or [2-^{13}C]pyruvate with a polarization of ~30% or ~20% respectively[17,24].

Hyperpolarized ^{13}C MRS protocol

On two separate days animals received either a [1-^{13}C]- or [2-^{13}C]pyruvate injection and MR scan, with at least one day between scans. A home-built ^{1}H/^{13}C butterfly coil (loop diameter, 20mm) was placed over the rat chest, localizing signal from the heart[17]. Rats were positioned in a 7T horizontal bore MR scanner interfaced to an Inova console (Varian Inc, Yarnton, UK). Correct positioning was confirmed by the acquisition of an axial proton fast low angle shot image. An ECG-gated shim was used to reduce the proton linewidth to ~120Hz. One ml of either hyperpolarized [1-^{13}C]- or [2-^{13}C]pyruvate was injected over 10s into the anesthetised rat. Sixty individual ECG-gated ^{13}C MR pulse-acquire cardiac spectra were acquired over one min after injection (TR, 1s; excitation flip angle, 5°; sweep width, 13,593Hz; acquired points, 2,048; frequency centred on the C1 pyruvate resonance).

^{13}C-MRS data analysis

All cardiac ^{13}C spectra were analysed using the AMARES algorithm in the jMRUI software package[29]. Spectra were DC offset-corrected based on the last half of acquired points. The peak areas of [1-^{13}C]pyruvate, [1-^{13}C] lactate, [1-^{13}C]alanine, [^{13}C]carbon dioxide ($^{13}CO_2$) and [^{13}C]bicarbonate (for [1-^{13}C]pyruvate) and [2-^{13}C]pyruvate, [1-^{13}C]acetylcarnitine, [1-^{13}C]citrate and [5-^{13}C]glutamate (for [2-^{13}C]pyruvate) at each time point were quantified and used as input data for a kinetic model. The kinetic model developed for the analysis of hyperpolarized [1-^{13}C] and [2-^{13}C]pyruvate MRS data is based on a model initially developed by Zierhut *et al.* (2010) and further developed by Atherton *et al.* (2011)[30,31].

The peak areas of *in vivo* $^{13}CO_2$ and [^{13}C]bicarbonate were also used to estimate intracellular pH (pH_i) in the heart. Using the method described by Schroeder *et al.* (2010)[32], two single 1s spectra were summed to increase signal to noise. The first 16 time points were then plotted to estimate pH_i[32].

Tissue collection

One day after hyperpolarized scans, animals were anaesthetized using an intraperitoneal injection of pentobarbital sodium (150mg/kg body weight, Euthatal, Merial, UK). The beating heart was rapidly removed and placed in ice cold phosphate buffered saline (PBS,

Sigma-Aldrich). A subset of hearts were perfused in the Langendorff mode to assess cardiac energetics using ^{31}Phosphorus (^{31}P) MRS and were therefore placed in ice cold Krebs buffer, instead of PBS. The remaining hearts were blotted (to remove liquid), freeze clamped and stored at −80°C for subsequent biochemical analysis.

^{31}P MRS

Six control and six SHR hearts were perfused using a retrograde Langendorff perfusion mode at 85 mmHg[33]. A dual tune ^{1}H/^{31}P volume coil was used for ^{31}P MRS on an 11.7T vertical bore MR scanner. Fully relaxed scans were performed to assess phosphocreatine (PCr), ATP, P_i and pH_i. Cardiac ^{31}P MR spectra were analysed using the AMARES algorithm in the jMRUI software package[29]. Absolute ^{31}P metabolite concentrations were calculated by assigning ATP concentrations ([ATP]) of 10.6mmol/L to the initial γ-ATP peak area for Wistar control hearts[34] and expressing all other ATP, PCr and P_i peak areas relative to this area[32,35]. pH_i was calculated from the P_i chemical shift[35], and this was compared with the *in vivo* pH_i derived from the ratio of $^{13}CO_2$ and [^{13}C]bicarbonate[32].

Western blotting

Protein expression of PDK (1, 2 and 4) and PDP (1 and 2) were measured in total heart homogenates from both SHR and Wistar control animals using SDS-PAGE and Western blotting [33]. Consistent protein loading was ensured by measuring protein concentration beforehand and confirmed using Ponceau staining of the membrane. All samples were run in duplicate on separate gels to confirm results. All data were normalized to control hearts.

Pyruvate dehydrogenase activity assay

PDH activity was measured using a spectrophotometric assay as previously described[18]. Briefly, this assay measures the proportion of the PDH enzyme in the active form and the maximal PDH activity. Activity is shown as μmoles NADH reduced per minute per gram wet weight (g.w.w.).

Statistics

All results are expressed as the mean ± SEM. Analysis for statistical significance was performed using an unpaired two-tailed Student's *t*-test assuming equal variance (SPSS, IBM, USA). Significance was taken at $p<0.05$.

Results

Hypertrophy and adaptive changes in cardiac function in the SHR heart

Cine-MRI was used to confirm the hypertrophic phenotype in the SHR animals. Left ventricular mass (LVM) was significantly increased by 56% in the SHR versus control (Table-1). This translated to a significant increase in the LVM to body weight ratio (53%), indicative of hypertrophy (Table-1, Figure-1). Cine-MRI was also used to assess *in vivo* cardiac function. Stroke volume and end diastolic volume were significantly increased by 19% and 18%, respectively, whilst heart rate was reduced by 18% in the SHR. This resulted

in no overall change in cardiac output or ejection fraction indicative of compensated hypertrophy.

A mid-papillary slice was selected to assess diastolic function using HTR-cine MRI. HTR-cine is able to assess filling of the LV following end systole[28]. Whilst the peak early filling rate was unaltered between groups (Figure-2A), the peak late filling rate, which represents atrial filling of the LV, was significantly reduced by ~0.3ml.s^{-1} in the SHR heart ($p<0.05$, Figure-2B).

In vivo PDH flux was increased in the SHR heart

^{13}C label incorporation into CO_2 and bicarbonate pools (PDH flux) was significantly increased by 85% in the SHR heart compared to control (Figure-3A). ^{13}C label incorporation into alanine was also significantly increased by 28%, whilst lactate labelling was unchanged between groups. To confirm the increase in ^{13}C label incorporation into CO_2 and bicarbonate, an *in vitro* biochemical assay was performed to measure PDH activity. Activity of the active PDH fraction in the SHR heart is significantly elevated from 0.8±0.2 to 1.8±0.3μmol.min^{-1}.g.w.w.$^{-1}$, an increase of 135% compared to control (Figure-3B). Maximal PDH activity was unchanged between groups (3.6±0.8 and 5.5±1.0μmol.min^{-1}.g.w.w.$^{-1}$, for controls and SHR hearts, respectively). This indicates PDH flux is increased in the SHR heart *in vivo* and that changes to ^{13}C label incorporation into CO_2 and bicarbonate are due to more of the enzyme being active rather than an increase in maximal PDH activity and content.

In vivo assessment of TCA cycle intermediates in the SHR heart

In the SHR heart, [2-^{13}C]pyruvate incorporation in the SHR heart was significantly increased by 72% into citrate, 118% into acetylcarnitine and 81% into glutamate compared to control (Figure-4A). As there was a significant increase in PDH flux, this increased ^{13}C label incorporation may be a result of more labelled acetyl-CoA being processed in to the TCA cycle. To correct for this increase in ^{13}C label flux, [2-^{13}C]pyruvate data was normalized to [1-^{13}C]pyruvate incorporation into bicarbonate+CO_2. Following normalization, no change to ^{13}C label incorporation was detected into either acetylcarnitine, glutamate or citrate pools (Figure-4B). Therefore the observed increase in [2-^{13}C]pyruvate label incorporation was relative to increased PDH flux and not greater flux in the TCA cycle.

Normal phosphate energetics and pH_i in the *in vitro* SHR heart

To assess high energy phosphate energetics in the heart, ^{31}P MRS was used performed on the perfused control and SHR hearts. In the control hearts, the average [ATP] was 10.6±1.2mmol/L, [PCr] was 16.4±2.7mmol/L and [P_i] was 1.9±0.3mmol/L (Figure-5). In the SHR hearts, the average [ATP] was 9.3±0.5mmol/L, [PCr] was 14.7±1.7mmol/L and [P_i] was 3.6±0.9mmol/L. [ATP], [PCr] and [P_i] were not significantly different between groups. This led to an average PCr/ATP ratio of 1.8±0.1 and 1.6±0.1, for control and SHR hearts respectively.

The estimated *in vivo* pH_i from the ^{13}C-MRS data was 7.12±0.02 and 7.14±0.02 for control and SHR, respectively. The pH_i measured from ^{31}P MRS was 7.06±0.01 and 7.06±0.02 for control and SHR, respectively, these data showed that there was no significant difference in cardiac intracellular pH between groups.

Increases in PDH flux are a result of changes in regulatory enzymes

To assess the regulatory state of PDH, western blots were performed on the key regulators of PDH in the heart: PDP(1 and 2) and PDK(1, 2 and 4). Assessment of PDK1 and 4 protein expression, showed that in the SHR heart there was a 26% and 25% reduction in protein expression, respectively, compared to control hearts (Figure-6). PDK2 was also reduced but not significantly (p=0.15). PDP1 protein expression showed a non-significant decrease (p=0.07), whilst PDP2 was significantly reduced by 29% between controls and SHR hearts (Figure-6).

Discussion

Extensive studies of the SHR heart have shown that after 15 weeks they develop concentric hypertrophy due to pressure overload[15,36]. *In vivo* measurements in this study using cine-MRI, have confirmed a 56% increase in left ventricular mass (LVM) and 53% increase in LVM to body weight ratio. Also *in vivo* cardiac functional data indicates that the 15 week SHR is an early disease model with hyperfunctional compensatory remodelling[37]. There are several key compensatory changes in function in the SHR compared with controls. Heart rate is significantly lower in the SHR, whilst stroke volume and end diastolic volume are significantly elevated. The result is that cardiac output and ejection fraction remain unchanged between groups, indicative of compensatory remodelling in response to the hypertension[37]. To accompany this, HTR cine-MRI showed that there was a significant reduction in peak late filling rate. This is hypothesised to be the rate of filling of the LV from the left atrium[28]. These data indicate a compensated hypertrophy disease stage in the 15 week SHR, with normalized cardiac function.

Further to compensated functional changes in the SHR, there are also several metabolic alterations which maintain normal energetics. *In vivo* assessment of SHR cardiac metabolism was performed using hyperpolarized ^{13}C MRS and highlighted several alterations. Firstly we demonstrate that the SHR heart has increased modulation of both *in vivo* PDH flux and AAT. This was detected as a significant increase in ^{13}C label incorporation between [1-^{13}C]pyruvate and [^{13}C]bicarbonate+$^{13}CO_2$ (PDH) and [1-^{13}C]alanine (AAT) in the *in vivo* hypertensive heart. An *in vitro* PDH activity assay was also employed to determine PDH activity, which was significantly elevated in the SHR heart, confirming hyperpolarized PDH flux data.

^{13}C label incorporation was also significantly increased into alanine, via AAT. These data suggest that in the SHR heart there is either a larger pool of free alanine in the tissue or an increase in AAT activity. There are several possible explanations for this increased ^{13}C label incorporation into alanine, which include export of cardiac alanine to the liver for the glucose-alanine cycle[38] or increased alanine production as would be required for the increase in protein synthesis characteristic of hypertrophy. Also, several papers have linked

the presence of alanine in the blood/urine to increases in blood pressure, so the observed increase here could be a consequence of the underlying hypertension[39,40].

The increase in PDH flux was coupled with an increase in ^{13}C label incorporation into citrate, acetylcarnitine and glutamate pools. No change was observed in ^{13}C label incorporation into the TCA cycle when label flux was normalized to flux through PDH. This implies that the apparent increases in citrate, acetylcarnitine and glutamate are derived from increased production of [2-^{13}C]acetyl-CoA, consistent with an increase in glucose oxidation. Furthermore, it was expected that the label incorporation from [1-^{13}C]pyruvate to [1-^{13}C]lactate would increase in the SHR heart, which would have implied a shift to a glycolytic phenotype, however this was not the case. Both these pieces of evidence highlight that the SHR has compensated cardiac metabolism, with a switch to greater glucose oxidation.

A defect in the LCFA transporter (FAT/CD36) has previously been identified in the SHR[11], which leads to a reduction in β-oxidation. Labarthe *et al.* (2005) have shown a significant reduction in ^{13}C label incorporation from [1-^{13}C]oleate, a LCFA, into the TCA cycle in the SHR[13]. They also stressed the importance of medium CFA (MCFA) in the SHR to compensate for the reduced contribution of LCFA to β-oxidation[13,41]. The defect in FAT/CD36 does not however, lead to a change in energetics in the heart. ^{31}P MRS can be used to determine cardiac energetics where significant alterations in [ATP] or/and [PCr] can indicate a mismatch in energy production in the heart. As *in vivo* cardiac ^{31}P MRS is particularly difficult due to sensitivity issues and cross contamination from other organs, the perfused heart was used to assess high energy phosphate energetics. Within the SHR heart [ATP] and [PCr] were not significantly different from controls hearts. This resulted in no significant difference in the PCr/ATP ratio, a measure of cardiac energetics within the heart. The SHR heart will be accustomed to higher arterial pressures and as the perfusion pressure was matched between the SHR and control animals, this may account for the absence of any difference in energetics [13]. However a previous study, measuring absolute concentrations of PCr and other high energy phosphates, observed no difference at 15 weeks of age in the SHR heart, but this balance was disturbed at the later timepoint of 25 weeks [9]. ^{31}P and ^{13}C MRS were also used here to determine the intracellular pH in the *in vitro* and *in vivo* heart, respectively[32]. These results indicate that the intracellular pH is unaltered between the SHR and control heart and the pH_i measurements were consistent with previously published data from the control Wistar heart[32]. This would imply normal aerobic metabolism and fits with no significant increase in the [1-^{13}C]lactate flux.

To further understand the mechanism behind the increase in PDH activity several key regulatory proteins were probed. PDKs are one of the major regulatory factors of PDH activity in the heart[19,42]. The PDK isoforms are activated by several mechanisms including hypoxia, increases in the end-products acetyl-CoA and NADH, and increases in β-oxidation[42-44]. PDKs can be activated short term by these factors or long term by transcriptional up regulation[19,44]. Here we observe a significant reduction in protein expression of PDK1 and PDK4 in the SHR heart compared to controls. Bowker-Kinley and colleagues have previously shown that PDK1 displays the highest specific activity and is highly sensitive to changes in the NAD^+:NADH ratio, which will be disturbed in the SHR,

due to the reduction in LCFA oxidation[11,42]. Our data indicates that the reduction in PDK1 and 4 protein expression might be sufficient to elicit the large increase in PDH flux and activity demonstrated here.

Other mechanisms for PDH modulation also exist including increased PDP activity and end product inhibition. Interestingly, protein expression data here show that PDP1 content did not increase but rather there was potentially a reduction, although not significant (p=0.07). This was accompanied by a significant decrease in the calcium insensitive PDP2 in the SHR heart. Whilst it seems counter intuitive that PDP1 and PDP2 protein expression would be decreased in the SHR heart, there may be compensatory alterations in activity. Elevated intracellular calcium ($[Ca^{2+}]_i$) and other cofactors (i.e. magnesium) have been shown to activate PDP, concurrently increasing PDH flux and the proportion of PDH in the active fraction[45]. Previous data from the left ventricle of SHRs, have shown a significantly elevated concentration of $[Ca^{2+}]_i$ compared to Wistar rats[36]. The final mechanism to consider is that the PDH increase is mediated by a reduction in end product inhibition. In the SHR heart there would be a reduction in acetyl-CoA and NADH derived from LCFA[13], this would reduce end product inhibition on PDH. Resulting in an increase in PDH flux. The current evidence suggests that increased PDH activity in the SHR heart is modulated by changes to PDK1 and 4 expression as well as a reduction in acetyl-CoA end product inhibition due to the reduced oxidation of LCFA.

The results of this study highlight the unique ability of hyperpolarized MRS to investigate *in vivo* alterations in cardiac metabolism seen in the diseased heart. Hyperpolarized MRS also offers the possibility to monitor animals at different time points during the development of disease and permits *in vivo* assessment where previously terminal techniques would have been required, i.e. biochemical analysis or the perfused heart[13,46]. The demonstration of *in vivo* metabolic alterations in animal models of cardiovascular diseases is made more relevant by the potential for future clinical application of this technology[47]. Clinical application of hyperpolarized MRS would allow direct, *in vivo* assessment of alterations in cardiac metabolism in a range of cardiovascular diseases. However the limitations of this technique should also be considered, for example the rapid decay of the hyperpolarized signal requires fast tracer production and injection. There is also a general requirement for injection of supraphysiological concentrations of the tracer. Although in the case of pyruvate, as used here, the physiological effect of the injection has been shown to be minimal with the increase in the plasma pyruvate concentration limited to 0.25mM, only slightly above the normal physiological level[16,24,48].

Conclusions

As expected, 15 week SHRs had significant hypertrophy which was accompanied by compensatory remodelling. Functional alterations in stroke volume, heart rate and the late diastolic filling rate were consistent with compensated hypertrophy. The use of *in vivo* hyperpolarized spectroscopy techniques in this study showed a significant increase in ^{13}C label incorporation through PDH into [^{13}C]bicarbonate+$^{13}CO_2$ and into the TCA cycle. Taken together with the [1-^{13}C]lactate data, this would suggest that there is an increase in glucose oxidation through PDH rather than an increase in anaerobic metabolism in the SHR

heart. Our work indicates a switch away from the classical, predominantly β-oxidation driven cardiac metabolism, matching evidence from previous *in vitro* data[13]. The genetic predisposition to reduced β-oxidation due to loss of CD36, may therefore drive the metabolic alterations seen in the SHR heart.

Acknowledgements

We would like to thank Mrs Vicky Ball and Miss Rosalind Bray for their technical assistance.

Sources of Funding

This work was supported by the British Heart Foundation. MSD was funded by a 4 year British Heart Foundation studentship in a BHF centre of Excellence [grant number: FS/08/067].

References

1. WHO. Global Health Observatory Data Repository [Internet]. [cited 2012 Feb 17];Available from: http://apps.who.int/ghodata/
2. Opie , LH. Heart physiology: from cell to circulation. 4. Lippincott Williams & Wilkins; Philadelphia: 2004.
3. Visscher MB, Mulder AG. The carbohydrate metabolism of the heart. Am J Physiol. 1930; 94:630–640.
4. Bing RJ, Siegel A, Ungar I, Gilbert M. Metabolism of the Human heart II. Studies on Fat, Ketone and Amino Acid Metabolism. Am J Med. 1954; 16:504–515. [PubMed: 13148192]
5. Randle PJ, Garland PB, Hales CN, Newsholme EA. The glucose fatty-acid cycle. Its role in insulin sensitivity and the metabolic disturbances of diabetes mellitus. The Lancet. 1963:1785.
6. Neubauer S. The failing heart--an engine out of fuel. New Engl J Med. Mar 15.2007 356:1140–1151. [PubMed: 17360992]
7. Ashrafian H, Redwood C, Blair E, Watkins H. Hypertrophic cardiomyopathy:a paradigm for myocardial energy depletion. Trends Genet. May.2003 19:263–268. [PubMed: 12711218]
8. Iemitsu M, Shimojo N, Maeda S, Irukayama-Tomobe Y, Sakai S, Ohkubo T, et al. The benefit of medium-chain triglyceride therapy on the cardiac function of SHRs is associated with a reversal of metabolic and signaling alterations. Am J Physiol - Heart C. 2008; 295:H136–144.
9. Shimamoto N, Goto N, Tanabe M, Imamoto T, Fujiwara S, Hirata M. Myocardial energy metabolism in the hypertrophied hearts of spontaneously hypertensive rats. Basic Res Cardiol. 1982; 77:359–357. [PubMed: 6216880]
10. McGuire PG, Twietmeyer TA. Aortic endothelial junctions in developing hypertension. Hypertension. 1985; 7:483–490. [PubMed: 4007987]
11. Aitman TJ, Glazier AM, Wallace CA, Cooper LD, Norsworthy PJ, Wahid FN, et al. Identification of Cd36 (Fat) as an insulin-resistance gene causing defective fatty acid and glucose metabolism in hypertensive rats. Nat. Genet. Jan.1999 21:76–83. [PubMed: 9916795]
12. Hajri T, Han XX, Bonen A, Abumrad NA. Defective fatty acid uptake modulates insulin responsiveness and metabolic responses to diet in CD36-null mice. J Clin Invest. 2002; 109:1381–1389. [PubMed: 12021254]
13. Labarthe F, Khairallah M, Bouchard B, Stanley WC, Des Rosiers C. Fatty acid oxidation and its impact on response of spontaneously hypertensive rat hearts to an adrenergic stress : benefits of a medium-chain fatty acid. Am J Physiol - Heart C. 2005; 288:1425–1436.
14. Hajri T, Ibrahimi A, Coburn CT, Knapp FF, Kurtz T, Pravenec M, et al. Defective fatty acid uptake in the spontaneously hypertensive rat is a primary determinant of altered glucose metabolism, hyperinsulinemia, and myocardial hypertrophy. J Biol Chem. Jun.2001 276:23661–23666. [PubMed: 11323420]
15. Rimbaud S, Sanchez H, Garnier A, Fortin D, Bigard X, Veksler V, et al. Stimulus specific changes of energy metabolism in hypertrophied heart. J Mol Cell Cardiol. Jun.2009 46:952–959. [PubMed: 19452634]

Europe PMC Funders Author Manuscripts

16. Atherton HJ, Schroeder MA, Dodd MS, Heather LC, Carter EE, Cochlin LE, et al. Validation of the in vivo assessment of pyruvate dehydrogenase activity using hyperpolarised (13)C MRS. NMR Biomed. Aug.2011 24:201–208. [PubMed: 20799252]
17. Schroeder MA, Cochlin LE, Heather LC, Clarke K, Radda GK, Tyler DJ. In vivo assessment of pyruvate dehydrogenase flux in the heart using hyperpolarized carbon-13 magnetic resonance. P Natl Acad Sci USA. Aug.2008 105:12051–12056.
18. Seymour AM, Chatham JC. The effects of hypertrophy and diabetes on cardiac pyruvate dehydrogenase activity. JMol Cell Cardiol. 1997; 29:2771–2778. [PubMed: 9344771]
19. Wu P, Sato J, Zhao Y, Jaskiewicz J, Popov KM, Harris RA. Starvation and diabetes increase the amount of pyruvate dehydrogenase kinase isoenzyme 4 in rat heart. Biochem J. 1998; 329:197–201. [PubMed: 9405294]
20. Paternostro G, Clarke K, Heath J, Seymour AM, Radda GK. Decreased GLUT-4 mRNA content and insulin-sensitive deoxyglucose uptake show insulin resistance in the hypertensive rat heart. Cardiovasc Res. Aug.1995 30:205–211. [PubMed: 7585807]
21. Ardenkjaer-Larsen JH, Fridlund B, Gram A, Hansson G, Hansson L, Lerche MH, et al. Increase in signal-to-noise ratio of > 10,000 times in liquid-state NMR. P Natl Acad Sci USA. Sep.2003 100:10158–10163.
22. Golman K, Ardenkjaer-Larsen JH, Petersson JS, Mansson S, Leunbach I. Molecular imaging with endogenous substances. P Natl Acad Sci USA. Sep.2003 100:10435–10439.
23. Golman K, Olsson LE, Axelsson O, Mansson S, Karlsson M, Petersson JS. Molecular imaging using hyperpolarized 13C. Br J Radiol. Dec.2003 76:S118–S127. [PubMed: 15572334]
24. Schroeder MA, Atherton HJ, Dodd MS, Lee P, Cochlin LE, Radda GK, et al. The Cycling of Acetyl-CoA through Acetylcarnitine Buffers Cardiac Substrate Supply: A Hyperpolarised 13C Magnetic Resonance Study. Circ Cardiovasc Imaging. 2012; 5:201–209. [PubMed: 22238215]
25. Schroeder MA, Atherton HJ, Ball DR, Cole MA, Heather LC, Griffin JL, et al. Real-time assessment of Krebs cycle metabolism using hyperpolarized 13C magnetic resonance spectroscopy. FASEBJ. Aug.2009 23:2529–2538.
26. Cassidy, PJ.; Schneider, JE.; Grieve, SM.; Lygate, CA.; Tyler, DJ.; Neubauer, S., et al. An animal handling system for small animals in vivo MR. ISMRM; 2005. p. 488(Abstract)
27. Tyler D, Lygate C, Schneider J, Cassidy P, Neubauer S, Clarke K. CINE-MR Imaging of the Normal and Infarcted Rat Heart Using an 11.7 T Vertical Bore MR System. J Cardiovasc Magn Res. May.2006 8:327–333.
28. Stuckey D, Carr C, Tyler D, Aasum E, Clarke K. Novel MRI method to detect altered left ventricular ejection and filling patterns in rodent models of disease. Magn Reson Med. Sep.2008 60:582–587. [PubMed: 18727095]
29. Naressi A, Couturier C, Castang I, de Beer R, Graveron-Demilly D. Java-based graphical user interface for MRUI, a software package for quantitation of in vivo/medical magnetic resonance spectroscopy signals. Comput Biol Med. 2001; 31:269–286. [PubMed: 11334636]
30. Zierhut ML, Yen Y-FF, Chen AP, Bok R, Albers MJ, Zhang V, et al. Kinetic modeling of hyperpolarized 13C1-pyruvate metabolism in normal rats and TRAMP mice. J Magn Reson. Jan. 2010 202:85–92. [PubMed: 19884027]
31. Atherton HJ, Dodd MS, Heather LC, Schroeder MA, Griffin JL, Radda GK, et al. Role of pyruvate dehydrogenase inhibition in the development of hypertrophy in the hyperthyroid rat heart: a combined magnetic resonance imaging and hyperpolarized magnetic resonance spectroscopy study. Circulation. Jun 7.2011 123:2552–2561. [PubMed: 21606392]
32. Schroeder MA, Swietach P, Atherton HJ, Gallagher FA, Lee P, Radda GK, et al. Measuring intracellular pH in the heart using hyperpolarized carbon dioxide and bicarbonate: a 13C and 31P magnetic resonance spectroscopy study. Cardiovasc Res. Apr 1.2010 86:82–91. [PubMed: 20008827]
33. Heather LC, Cole MA, Lygate CA, Evans RD, Stuckey DJ, Murray AJ, et al. Fatty acid transporter levels and palmitate oxidation rate correlate with ejection fraction in the infarcted rat heart. Cardiovascr Res. Dec 1.2006 72:430–437.
34. Cross HR, Clarke K, Opie LH, Radda GK, Heart I, Town C. Young Investigator Finalist from 1994 ISHR European Section Meeting Is Lactate-induced Myocardial Ischaemic Injury Mediated by

Decreased pH or Increased Intracellular Lactate ? J Mol Cell Cardiol. 1995; 27:1369–1381. [PubMed: 7473783]

35. Murray AJ, Lygate CA, Cole MA, Carr CA, Radda GK, Neubauer S, et al. Insulin resistance, abnormal energy metabolism and increased ischemic damage in the chronically infarcted rat heart. Cardiovasc Res. Jul 1.2006 71:149–157. [PubMed: 16616054]
36. Cuneo ME, Grassi de Gende AO. Cardiac sarcoplasmic reticulum characteristics in hypertrophic hearts from spontaneously hypertensive rats. Basic Res Cardiol. 1988; 83:286–295. [PubMed: 2843160]
37. Meerson FZ. Compensatory Hyperfunction of the Heart and Cardiac Insufficiency. Circ Res. 1962; X:250–258. [PubMed: 14472098]
38. Felig P, Pozefsky T, Marliss E, Cahill GF. Alanine: Key Role in Gluconeogenesis. Science. 1970; 167:1003–1004. [PubMed: 5411169]
39. Conlay LA, Maher TJ, Wurtman RJ. Alanine increases blood pressure during hypotension. Pharmacol Toxicol. May.1990 66:415–416. [PubMed: 2371250]
40. Holmes E, Loo RL, Stamler J, Bictash M, Yap IKS, Chan Q, et al. Human metabolic phenotype diversity and its association with diet and blood pressure. Nature. May 15.2008 453:396–400. [PubMed: 18425110]
41. Lauzier B, Merlen C, Vaillant F, McDuff J, Bouchard B, Beguin PC, et al. Post-translational modifications, a key process in CD36 function: lessons from the spontaneously hypertensive rat heart. JMol Cell Cardiol. Jul.2011 51:99–108. [PubMed: 21510957]
42. Bowker-Kinley MM, Davis WI, Wu P, Harris RA, Popov KM. Evidence for existence of tissue-specific regulation of the mammalian pyruvate dehydrogenase complex. Biochem J. 1998; 329:191–196. [PubMed: 9405293]
43. Huang B, Wu P, Bowker-Kinley MM, Harris RA. Regulation of pyruvate dehydrogenase kinase expression by peroxisome proliferator-activated receptor-alpha ligands, glucocorticoids, and insulin. Diabetes. Feb.2002 51:276–283. [PubMed: 11812733]
44. Kim, J-whan; Tchernyshyov, I.; Semenza, GL.; Dang, CV. HIF-1-mediated expression of pyruvate dehydrogenase kinase: a metabolic switch required for cellular adaptation to hypoxia. Cell Metabolism. Mar.2006 3:177–185. [PubMed: 16517405]
45. Denton RMM, Randle PJ, Martin BR. Stimulation by Calcium Ions of Pyruvate Dehydrogenase Phosphate Phosphatase. Biochem J. 1972; 128:161–163. [PubMed: 4343661]
46. Christe M, Rodgers RL. Altered glucose and fatty acid oxidation in hearts of the spontaneously hypertensive rat. J Mol Cell Cardiol. 1994; 26:1371–1375. [PubMed: 7869397]
47. Schroeder MA, Clarke K, Neubauer S, Tyler DJ. Hyperpolarized magnetic resonance: a novel technique for the in vivo assessment of cardiovascular disease. Circulation. Oct 4.2011 124:1580–1594. [PubMed: 21969318]
48. Schroeder MA, Atherton HJ, Cochlin LE, Clarke K, Radda GK, Tyler DJ. The Effect of Hyperpolarized Tracer Concentration on Myocardial Uptake and Metabolism. Magn Reson Med. 2009; 61:1007–1014. [PubMed: 19253408]

Europe PMC Funders Author Manuscripts

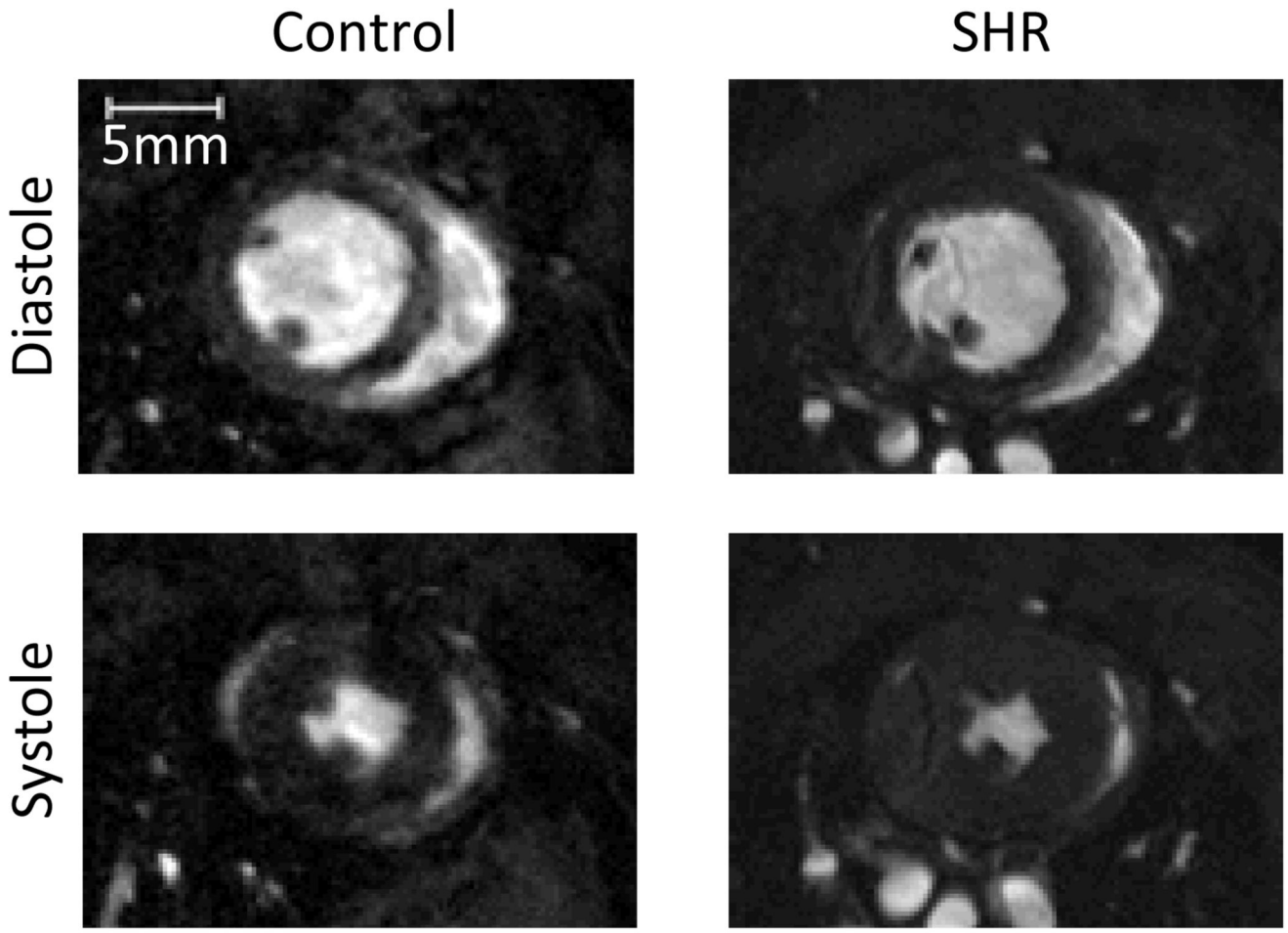

Figure-1.

A typical mid-papillary MR image of the control and SHR heart, during diastole and systole. Significant hypertrophy of the SHR heart can be seen compared to the control heart.

Europe PMC Funders Author Manuscripts

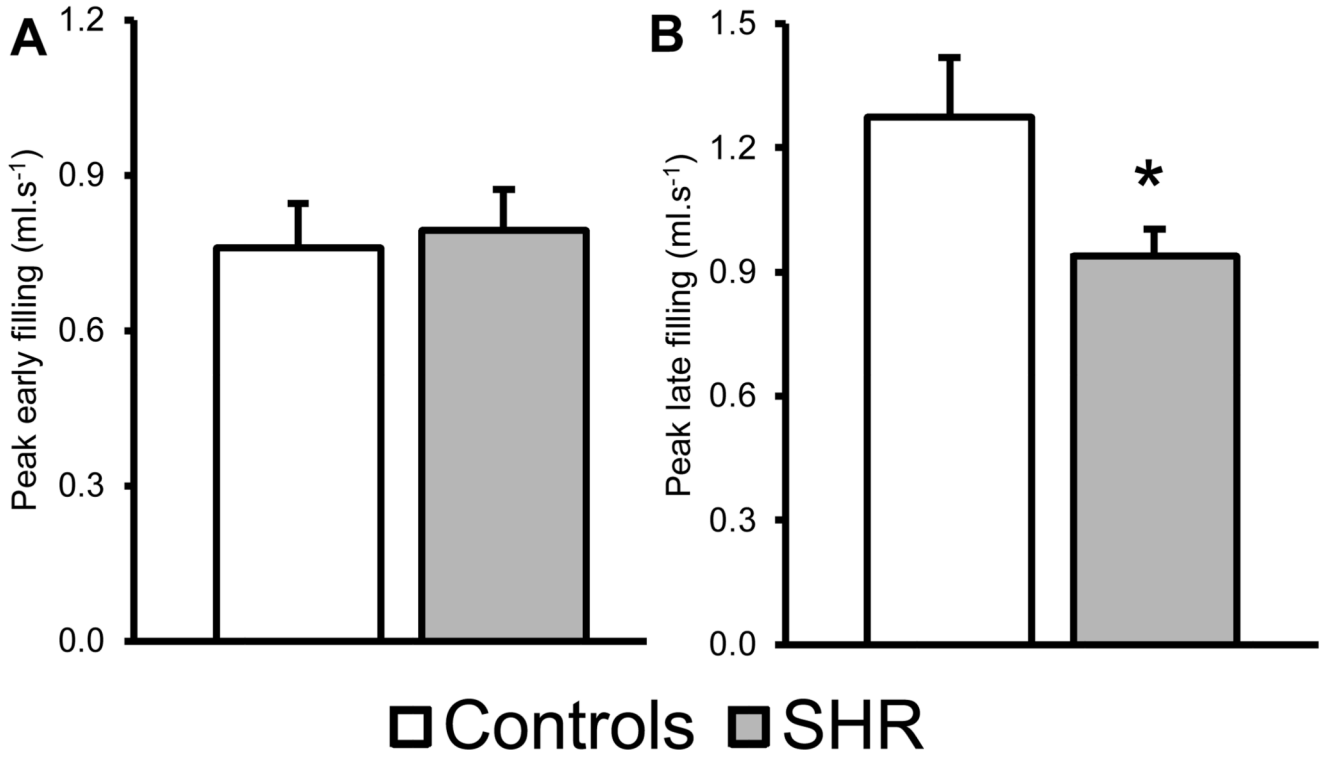

Figure-2. High Temporal Resolution cine-MRI was used to assess diastolic function

A) No change is seen in the peak early filling rate. B) A significant decrease in peak late filling rate (panel B) was seen in SHRs. * : $p<0.05$

Europe PMC Funders Author Manuscripts

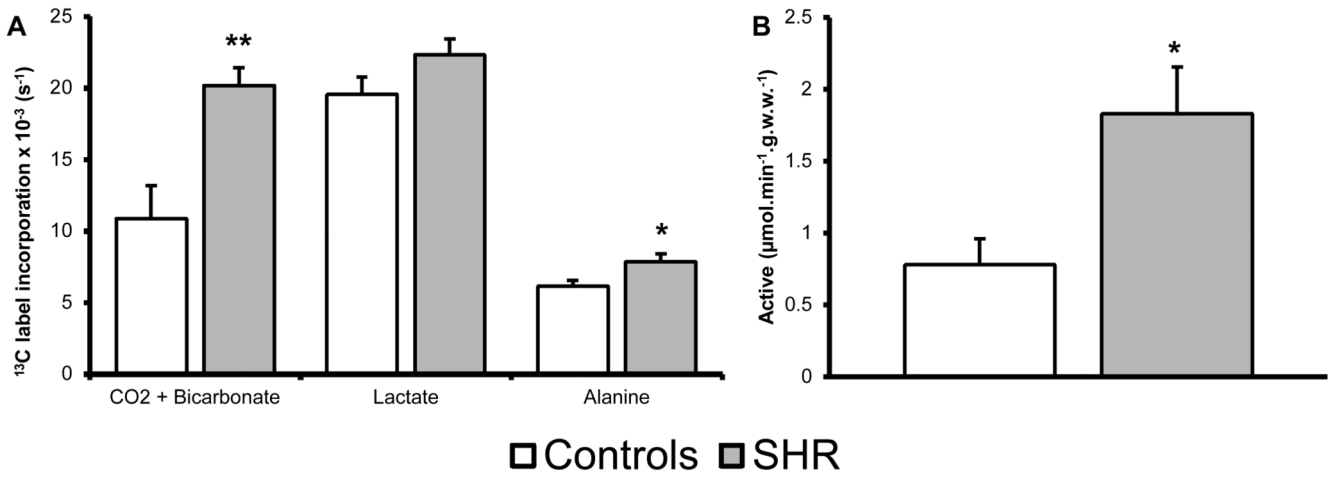

Figure-3. Assessed flux using [1-^{13}C]pyruvate and PDH activity

A) Hypertensive rats show an increase in ^{13}C label incorporation through PDH (CO_2 + bicarbonate) and through AAT (alanine), whilst there is no change to LDH (lactate). B) PDH activity assay, showing activity of active PDH fraction. Significant increase is seen in the activity of PDH in the SHR compared to control. *: $p<0.05$, **: $p<0.01$

Europe PMC Funders Author Manuscripts

Europe PMC Funders Author Manuscripts

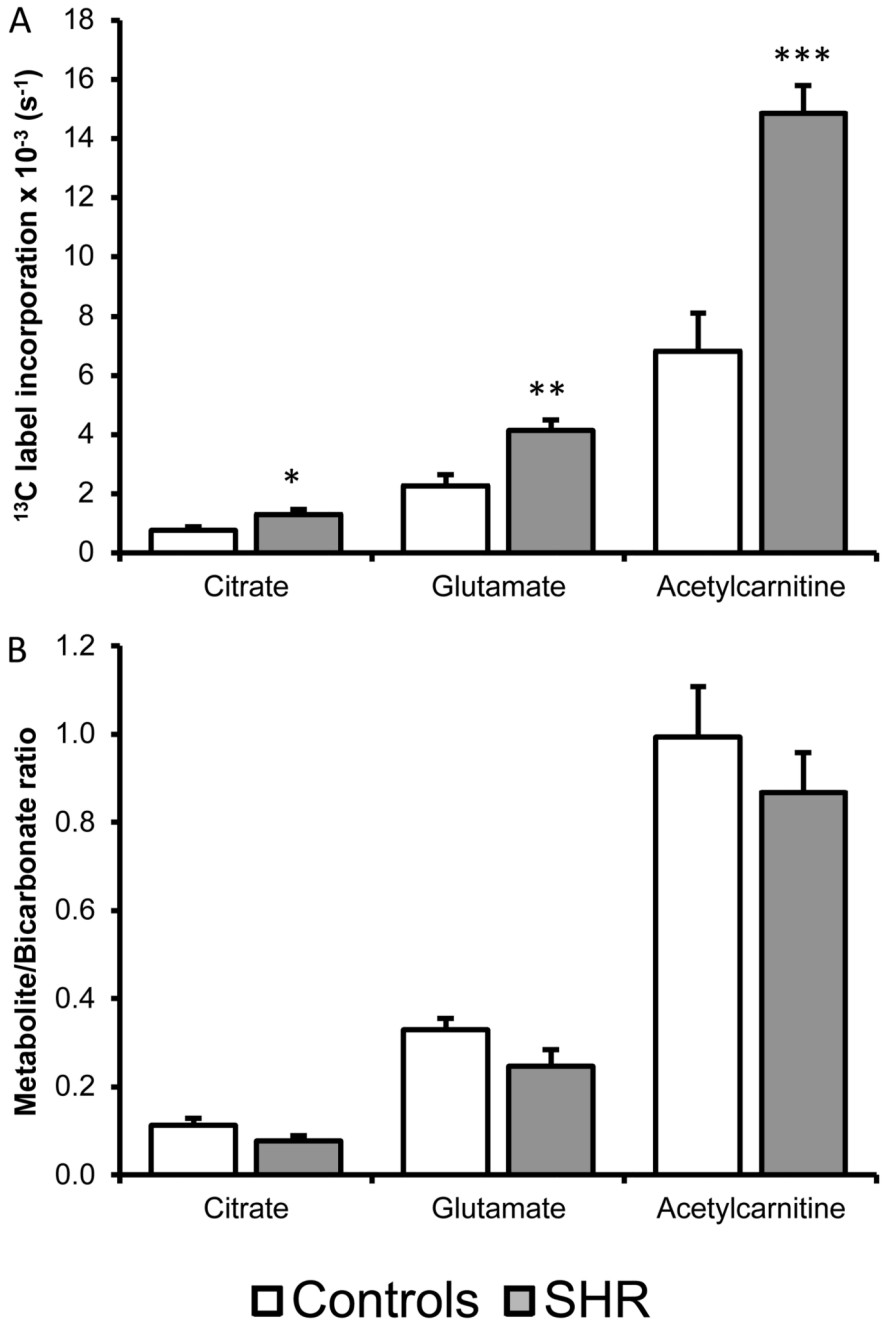

Figure-4. Assessed flux using [2-^{13}C]pyruvate

A) Hypertensive rats show an increase in label incorporation into the citrate, glutamate and acetylcarnitine pools. *: $p<0.05$, **: $p<0.01$, ***:$p<0.001$. B) [2-^{13}C]pyruvate data normalized to label flux through PDH.

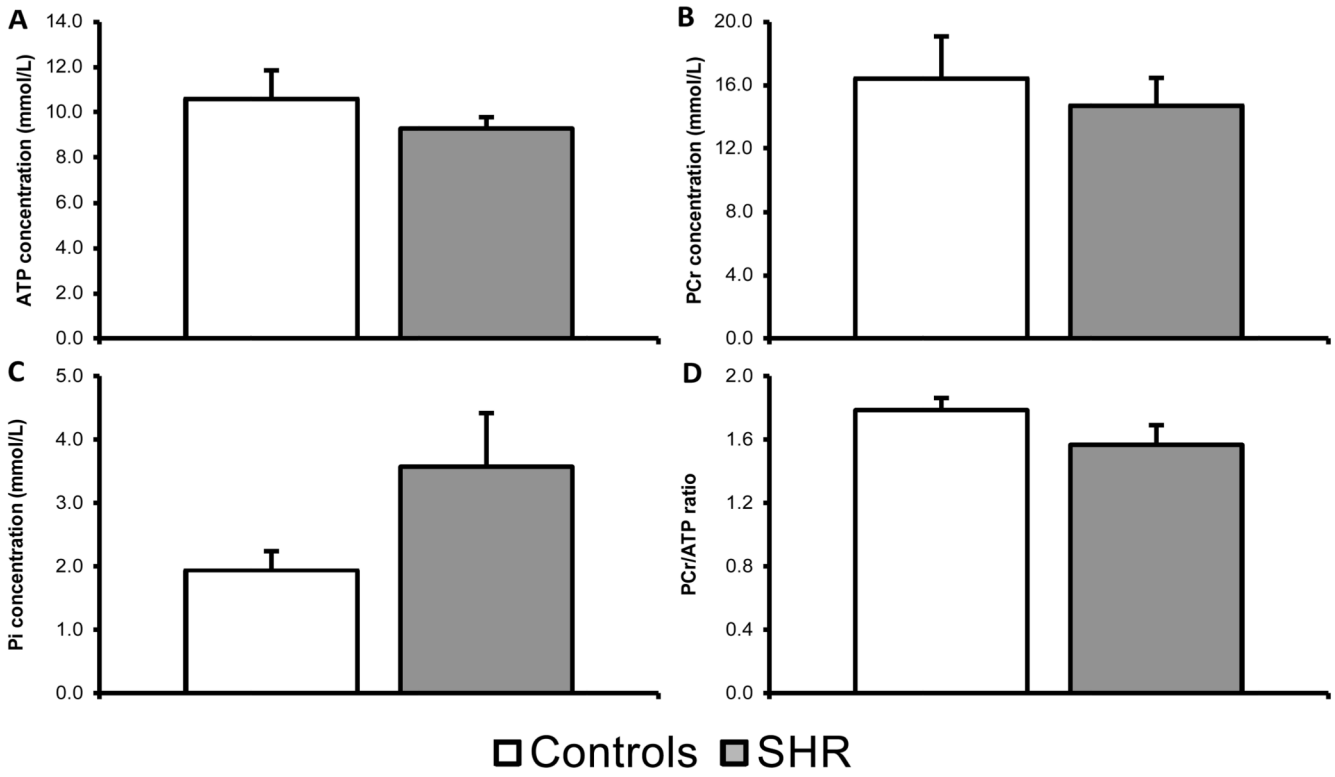

Figure-5. ^{31}P MRS of the *in vitro* heart

High energy phosphate energetics in the SHR and control heart are unaltered as represented by a normal [ATP], [PCr], [P_i] and PCr/ATP ratio.

Europe PMC Funders Author Manuscripts

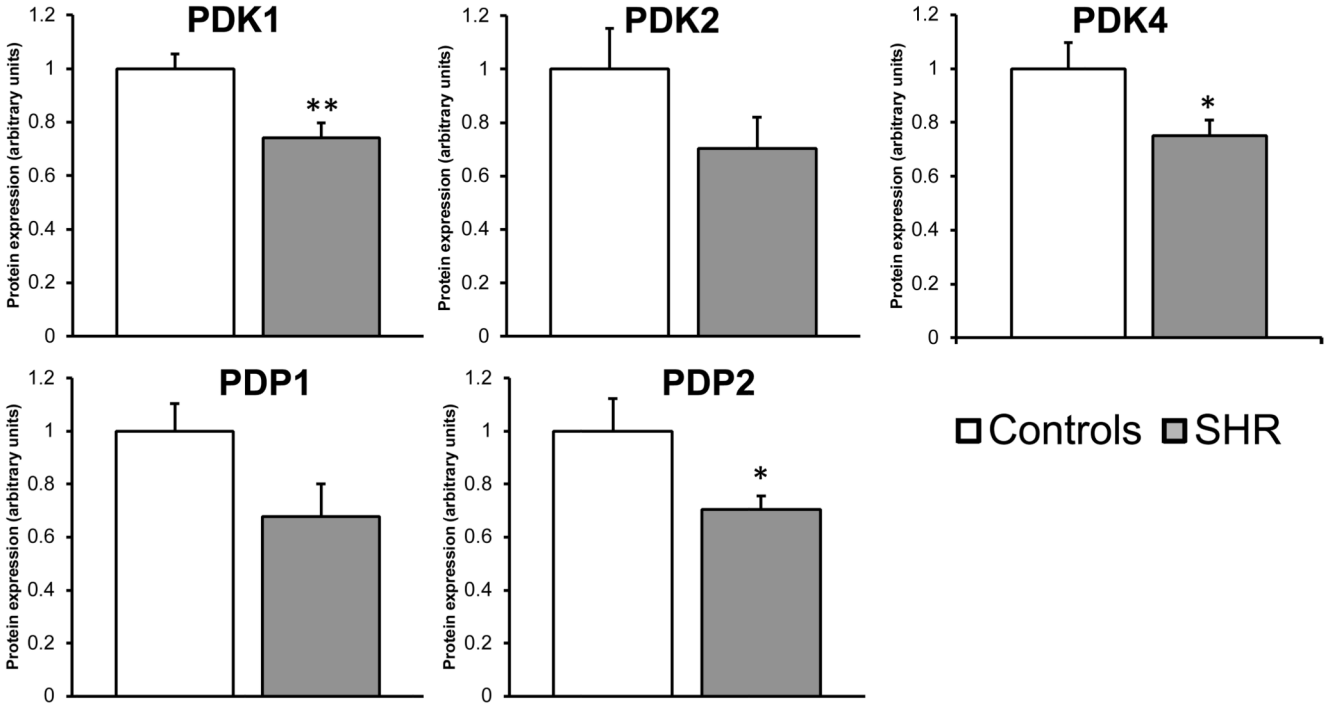

Figure-6. Altered protein expression of the PDKs and PDP2 in the SHR heart

To assess regulatory state of PDH, PDK1, PDK2, PDK4, PDP1, and PDP2 protein expression was measured. PDK1 and PDK4 expression was significantly reduced in the SHR heart compared to control. No significant alteration in protein expression was observed in PDP1 ($p=0.07$), however PDP2 was significantly decreased. *: $p<0.05$ **: $p<0.01$, data displayed as relative expression compared to control (arbitrary units).

Europe PMC Funders Author Manuscripts

Europe PMC Funders Author Manuscripts

Table-1

Function data from cine-MRI

	LVM (mg)	Body weight (g)	LVM/BW (mg.g^{-1})	Heart Rate (BPM)	Stroke Volume ($_{\mu}$l)	End diastolic volume (µl)	Cardiac Output (ml.min^{-1})	Ejection fraction (%)
Control	540 ± 20	306 ± 10	1.77 ± 0.04	419 ± 7	261 ± 16	325 ± 19	105 ± 6	81 ± 1
SHR	**840 ± 20** ***	312 ± 5	**2.71 ± 0.06** ***	**343 ± 14** ***	**310 ± 14** *	**382 ± 19** *	104 ± 5	81 ± 2

A significant decrease in heart rate was observed in the SHR, with an increase in stroke volume. Ejection fraction and cardiac output were unchanged between the SHR and control hearts. Values are mean data with S.E.M. Two-tailed Student t-test

* $p<0.05$,

*** $p<0.001$.